ORIGINAL ARTICLE

Pembrolizumab for anaplastic thyroid cancer: a case study

Marra Jai Aghajani[1,2] · Adam Cooper[2,3] · Helen McGuire[4,5] · Thomas Jeffries[6,7] · Jawad Saab[8] · Kasim Ismail[2,8] · Paul de Souza[1,2,9] · Victoria Bray[3] · Barbara Fazekas de St Groth[4,5] · Navin Niles[1,2,10,11] · Tara Laurine Roberts[1,2,9]

Abstract

Blockade of the PD-1/PD-L1 pathway with targeted monoclonal antibodies has demonstrated encouraging anti-tumour activity in multiple cancer types. We present the case of a patient with *BRAF*-negative stage IVC anaplastic thyroid cancer (ATC) treated with the anti-PD-1 monoclonal antibody, pembrolizumab, following radiographic progression on chemoradiation. Blood samples were collected prior to and at four time points during treatment with pembrolizumab. Mass cytometry was used to determine expression of relevant biomarkers by peripheral blood mononuclear cells. Faecal samples were collected at baseline and 4 weeks following treatment initiation; taxonomic profiling using 16S ribosomal RNA (rRNA) gene sequencing was performed. Following treatment, a marked expansion in CD20$^+$ B cell, CD16$^+$ CD56^{lo} NK cell and CD45RO$^+$ CCR7$^+$ central memory CD4$^+$ T-cell populations was observed in the peripheral blood. Proportions of cells expressing the co-receptors TIGIT, OX40 and CD86 also increased during treatment. A high abundance of bacteria of the order *Bacteroidales*, specifically from the *Bacteroidaceae* and *Rikenellaceae* families, was identified in the faecal microbiota. Moreover, the patient's microbiome was enriched in *Clostridiales* order members *Ruminococcaceae*, *Veillonellaceae* and *Lachnospiraceae*. Alpha diversity of the gut microbiome was significantly higher following initiation of checkpoint therapy as assessed by the Shannon and Simpson index. Our results suggest that treatment with pembrolizumab promotes expansion of T-, B- and NK cell populations in the peripheral blood at the time of tumour regression and have the potential to be implemented as predictive biomarkers in the context of checkpoint blockade therapy. Larger studies to confirm these findings are warranted.

Keywords Anti-PD-1 antibody · Pembrolizumab · Checkpoint inhibitor · Anaplastic thyroid cancer (ATC)

Abbreviations

AJCC	American Joint Committee on Cancer
ATC	Anaplastic thyroid cancer
BBB	Blood–brain barrier
Bregs	Regulatory B cells
CNS	Central nervous system
CONCERT	Centre for Oncology Education and Research Translation
CT	Computed tomography

✉ Marra Jai Aghajani
17691938@student.westernsydney.edu.au

1 Ingham Institute for Applied Medical Research, 1 Campbell St, Liverpool, NSW 2170, Australia

2 School of Medicine, Western Sydney University, Campbelltown, NSW, Australia

3 Liverpool Cancer Therapy Centre, Corner of Goulburn and Elizabeth Streets, Liverpool, NSW 2170, Australia

4 Discipline of Pathology, Faculty of Medicine and Health, University of Sydney, Sydney, NSW, Australia

5 Ramaciotti Facility for Human Systems Biology, Charles Perkins Centre, University of Sydney, Sydney, NSW, Australia

6 Hawkesbury Institute for the Environment, Western Sydney University, Penrith, NSW, Australia

7 School of Science and Health, Western Sydney University, Penrith, NSW, Australia

8 Sydney South West Pathology Services, Liverpool Hospital, Liverpool, NSW, Australia

9 South West Sydney Clinical School, UNSW Sydney, Sydney, NSW, Australia

10 Department of Head and Neck Surgery, Liverpool Hospital, Liverpool, NSW, Australia

11 Department of Clinical Medicine, Faculty of Medicine and Health Sciences, Macquarie University, Sydney, NSW, Australia

CTC	Circulating tumour cells
EBRT	External beam radiation therapy
FDG	Fluorodeoxyglucose
FNA	Fine needle aspiration
HL	Hodgkin's lymphoma
IMRT	Intensity-modulated radiation therapy
irAEs	Immune-related adverse events
MMT	Multimodal therapy
NLR	Neutrophil:lymphocyte ratio
pDCs	Plasmacytoid dendritic cells
PET/CT	Positron emission tomography/computed tomography
RCC	Renal cell carcinoma
sOTUs	Individual sequence variants
Tfh	Follicular T-helper cells
TPS	Tumour proportion score
WBRT	Whole-brain radiation therapy

Introduction

Anaplastic thyroid cancer (ATC) is a rare, undifferentiated carcinoma, with an annual incidence of 1–2 cases per million people worldwide [1]. Whilst accounting for less than 2% of thyroid cancers, ATC contributes to more than 50% of thyroid cancer-associated deaths [2]. Patients have a median survival of 3–5 months following diagnosis, and mortality rate of over 90% [3, 4]. Distant metastases are found in nearly 50% of patients at diagnosis, and a further 25% of patients develop metastases during disease progression [5]. The lung is the most common metastatic site (78%), followed by the intrathoracic lymph nodes (58%), neck lymph nodes (51%), pleura (29%), adrenal glands (24%), liver (20%), and brain (18%) [6].

Management of ATC consists of surgical resection of the primary tumour in those with localised disease, followed by high-dose external beam radiation therapy (EBRT) with or without concurrent radio-sensitising chemotherapy for curative intent [7]. Nonsurgical palliative treatment consisting of EBRT with or without concurrent chemotherapy can be offered to patients with unresectable disease [8]. However, substantial therapy-related toxicities arise following multimodal therapy (MMT), and patients with AJCC (also referred to as TNM) stage IVC disease derive limited benefit from even the most aggressive therapeutic approaches [9].

Programmed cell death protein 1 (PD-1) is an inhibitory molecule expressed on activated immune cells, including dendritic cells (DC), natural killer (NK) cells, monocytes, B cells, and T cells [10]. Binding of PD-1 to its ligand, programmed cell death ligand 1 (PD-L1) suppresses the cytolytic activity and potentiates the apoptosis of $CD8^+$ T cells [11]. Checkpoint inhibitors targeting the PD-1/PD-L1 pathway are efficacious in a range of cancers including non-small

cell lung cancer (NSCLC), melanoma, and renal cell cancer (RCC) [12]. However, only a fraction of patients benefit from anti-PD-1/PD-L1 monotherapies, with objective responses ranging from 5% to 55% [13].

Recent studies of PD-1/PD-L1 checkpoint blockade in the treatment of ATC have garnered mixed results. In a series of 12 ATC patients treated with salvage pembrolizumab after progression on kinase inhibitors, 42% demonstrated a partial response and 33% experienced stable disease [14]. An exceptional response was reported in a *BRAF* mutant and PD-L1-positive ATC patient treated with the anti-PD-1 antibody nivolumab following progression on the *BRAF* inhibitor vemurafenib [15]. The patient remained in complete radiographic and clinical remission 20 months after starting treatment. An overall response rate of 17% was observed in 30 ATC patients treated with single-agent spartalizumab, a PD-1-directed mAb [16]. Moreover, in a phase 2 study, all 3 patients died less than 6 months following treatment with pembrolizumab combined with docetaxel/doxorubicin and intensity-modulated radiation therapy (IMRT) [17], a disappointing survival outcome when compared to historical control methods. Several clinical trials investigating PD-1/PD-L1 inhibitors as monotherapy or in combination in ATC are presently underway (NCT02688608, NCT03211117, NCT03246958, NCT03181100). Currently, assessment of tumoral PD-L1 expression via immunohistochemistry (IHC) is the most widely implemented biomarker; however, its predictive capabilities are limited, with patients who express no or low tumoral PD-L1 experiencing long-term benefit [18–20] and patients with high PD-L1 unresponsive to treatment [21]. Tumour mutational load, mismatch repair deficiency, peripheral blood markers and the gut microbiota have been explored as alternate predictors of treatment response [22]. Further research establishing comprehensive biomarker panels is necessary to improve patient outcomes.

Here we present the case of a patient with *BRAF*-negative stage IVC ATC who demonstrated a response to checkpoint immunotherapy (anti-PD-1, pembrolizumab), and an analysis of candidate biomarkers.

Patient history

A 53-year-old man with previous asbestos exposure and a 50-pack year smoking history presented with a right-sided chest wall mass in May 2017. The patient underwent a computed tomography (CT) scan of the chest, which showed right pleural effusion and a soft tissue mass involving the right chest wall between the 8th and 9th ribs, 2.8 cm in width. There was also evidence of slight fullness of the left lobe of the thyroid gland. Six weeks later, a biopsy of the chest wall lesion revealed extensive tumour necrosis with a malignant spindle cell neoplasm, markedly pleomorphic

nuclei and frequent mitosis. A fine needle aspiration (FNA) biopsy of the thyroid nodule was suspicious for a neoplasm with highly atypical features. A diagnosis of sarcomatoid mesothelioma was favoured.

A positron emission tomography/computed tomography (PET/CT) staging scan was performed, demonstrating intense fluorodeoxyglucose (FDG) accumulation in the 6.0×4.0 cm soft tissue mass on the right chest wall. There was also intense FDG uptake in a large mass in the left lobe of the thyroid gland measuring 4.1×2.6 cm and in the right upper abdominal wall. A magnetic resonance imaging (MRI) scan confirmed these findings. These radiological findings were incongruent with the diagnosis of mesothelioma, particularly as the chest wall lesion appeared to arise from the muscle and not the pleura.

A biopsy of the left lobe of the thyroid revealed a hypercellular tumour with strong vimentin and cytokeratin AE 1/AE 3 positivity, and thyroglobulin, p63, calretinin and CK5/6 negativity, which is immunophenotypically inconsistent with mesothelioma. The thyroid biopsy was cytologically identical to the core biopsy of the right anterior chest wall lesion, both being of a spindle cell malignancy with cytokeratin immunopositivity. A diagnosis of ATC with distant chest and abdominal wall metastases was made.

The patient completed high-dose palliative radiation to the thyroid (50 Gray in 20 fractions) and chest wall (40 Gray in 15 fractions) with three doses of concurrent weekly doxorubicin (10 mg/m^2), which was complicated by dehydration, malnourishment, fatigue and pharyngolaryngitis. Six weeks after starting treatment, the patient demonstrated radiographic progression in the lungs and thyroid. IHC staining of the thyroid biopsy revealed an absence of the *BRAF V600E* mutation and very high tumoral PD-L1 positivity, with a tumour proportion score (TPS) of 100% (Fig. 1a, b). Given the strong PD-L1 expression, four doses of pembrolizumab (200 mg) was administered through a compassionate access protocol from the 10th January to the 30th March 2018.

A CT chest scan on the 19th of January revealed multiple pulmonary nodules, moderate right pleural effusion and approximately 20 hepatic metastases (Fig. 2a, b). After 1 month of pembrolizumab therapy, a follow-up CT showed a reduction in size of a lung nodule (8 mm, previously 12 mm in size), the right hilar lymph node (22×20 mm, previously 30×24 mm) and the largest of the hepatic metastases

Fig. 1 Immunohistochemical (IHC) analysis of PD-L1, CD4+, CD8+ and CD20+ in patient tumour biopsies. **a**, **b** IHC staining for PD-L1 (brown) on chest wall biopsy. **c** IHC staining for PD-L1 (brown) on small bowel biopsy. **d** IHC staining for CD8$^+$ on small bowel biopsy. **e** IHC staining for CD4$^+$ on small bowel biopsy. **f** IHC staining for CD20$^+$ on small bowel biopsy. Positive staining was visualized with DAB (brown colour indicates positivity) and counterstaining was performed with hematoxylin. Magnification is indicated in each frame
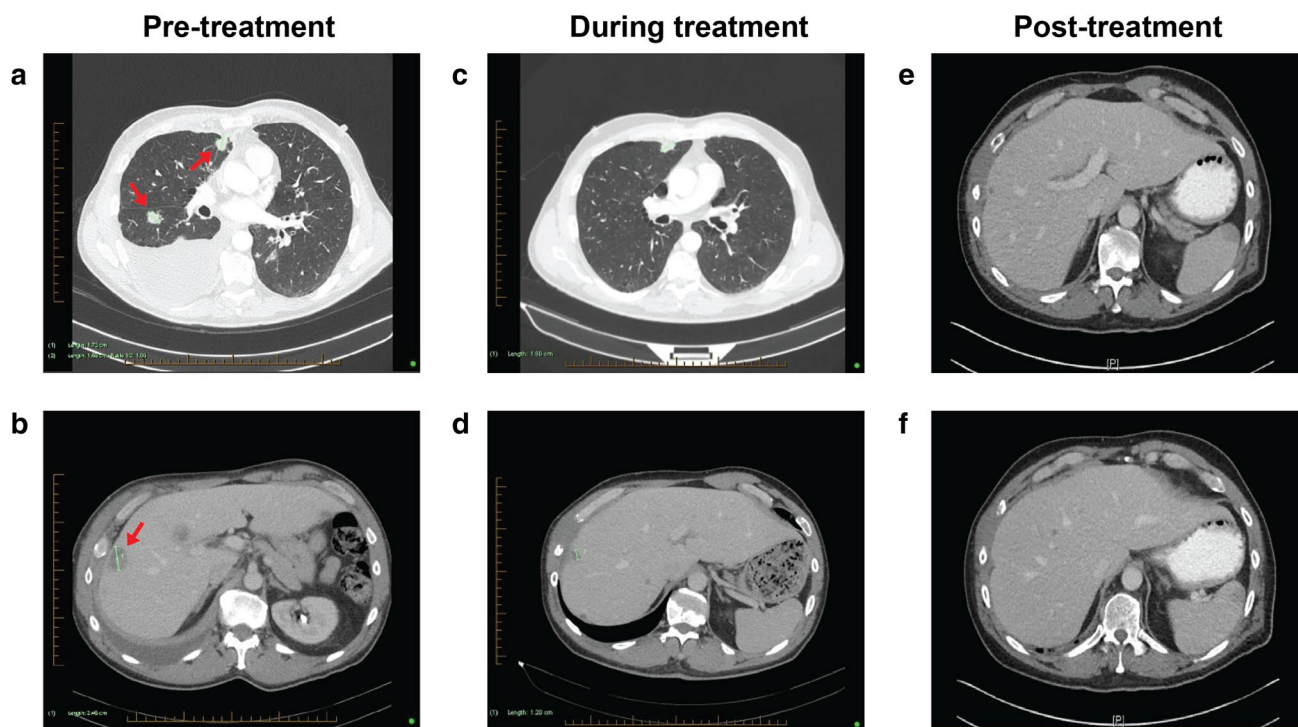
Pre-treatment **During treatment** **Post-treatment**
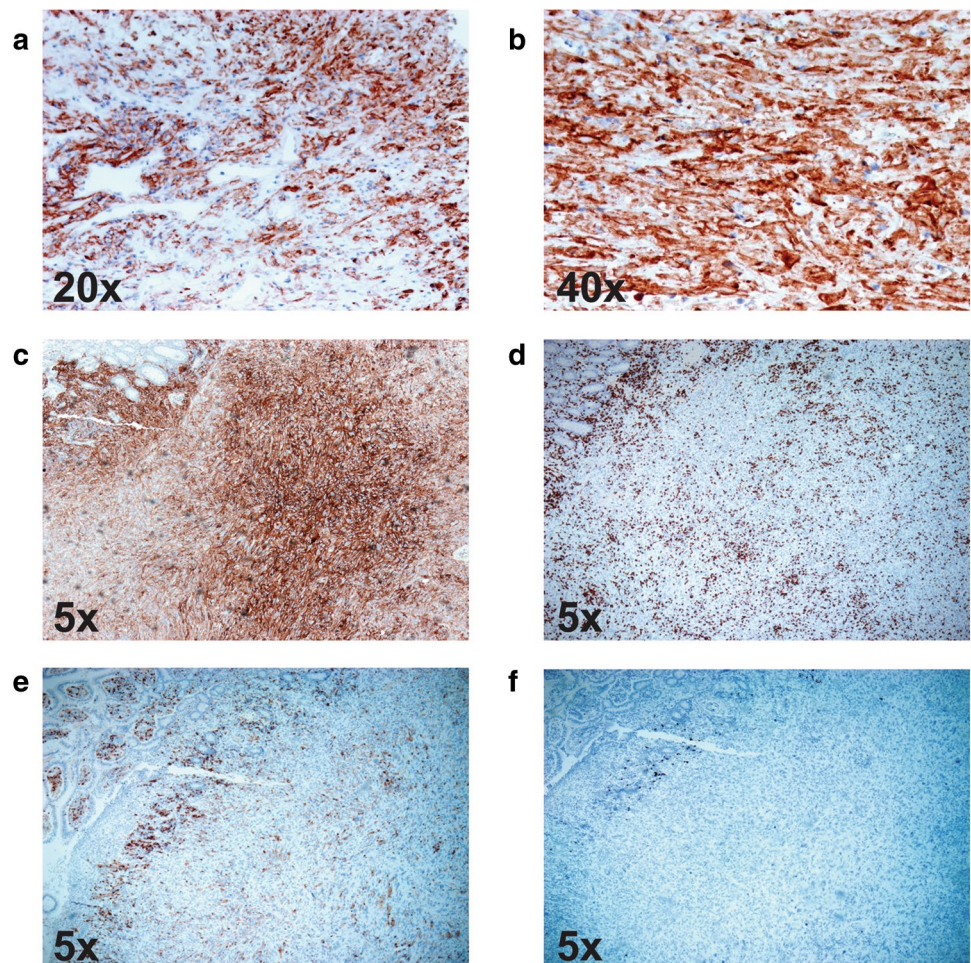
Fig. 2 Imaging of major tumour sites through patient journey. **a** Pre-treatment CT demonstrating multiple pulmonary nodules and right pleural effusion. **b** Pre-treatment CT showing the largest (25 mm) of 20 hepatic metastases. **c** Follow-up CT demonstrating a reduction in size of pulmonary nodules and near-complete resolution of right pleural effusion. **d** Follow-up CT showing a reduction in size of the largest hepatic metastasis. **e, f** Follow-up CT demonstrating a reduction in size of the largest hepatic metastasis (10 mm, previously 25 mm). Arrows point towards nodules in initial scan

(17 mm, previously 25 mm) (Fig. 2d). The right pleural effusion was resolving, with no new pulmonary nodules identified (Fig. 2c). A 53% reduction in total tumour burden was observed. A follow-up CT-guided biopsy of his lung nodule on the 30th May revealed a necrotic focus and presence of mesothelial cells, suggestive of therapeutic response to the anti-PD-1 therapy.

Three months after completing immunotherapy, a brain CT revealed multiple lesions indicative of cerebral metastases (Fig. 3c, d). A CT performed in December 2017 had detected no intra- or extra-axial brain metastases (Fig. 3a, b). The patient completed a course of palliative whole-brain radiotherapy on the 26th of June and was placed on dexamethasone.

On the 17th of August, a CT revealed a contained perforation into the small bowel. IHC of the small bowel resection confirmed metastatic ATC containing large areas of necrosis with secondary small bowel perforation. Many CD8$^+$ T cells were present within the tumour (Fig. 1d), with CD4$^+$ (Fig. 1e) and B cells (Fig. 1f) present to a lesser extent. PD-L1 was strongly expressed within the metastatic deposit, having a TPS of 100% (Fig. 1c). The CT revealed that the liver metastases had further reduced in size (< 10 mm)

(Fig. 3e, f). A repeat brain CT on the 17th of August demonstrated stable disease with no new lesions identified.

Despite the ongoing extracranial response and stable intracranial lesions on imaging following immunotherapy and whole-brain radiation therapy (WBRT), the patient's condition continued to deteriorate. He was transferred to a palliative care unit, where he passed away on the 23rd of September (9 months after commencing immunotherapy and 16 months from his initial presentation).

Materials and methods

Study subjects and samples

Peripheral blood mononuclear cells (PBMCs) were isolated from EDTA-treated whole blood using Ficoll-Paque Plus (GE Healthcare, Uppsala, Sweden) and cryopreserved in vapour-phase liquid nitrogen. The results collected from the case study patient were compared to a cohort of nine healthy age- and gender-matched controls with a median age of 58. These controls provided information on the range of values in the healthy population.

Fig. 3 Brain imaging prior to and following pembrolizumab treatment. Brain CT performed in December 2017 with no intra- or extra-axial brain metastases (**a**, **b**). Brain imaging of patient on the 7th June 2018 (**c**, **d**) showing multiple contrast-enhancing intraparenchymal mass lesions consistent with cerebral metastases. There is surrounding vasogenic oedema and local mass effect with a 4-mm midline shift towards the right. Arrows point towards mass lesions
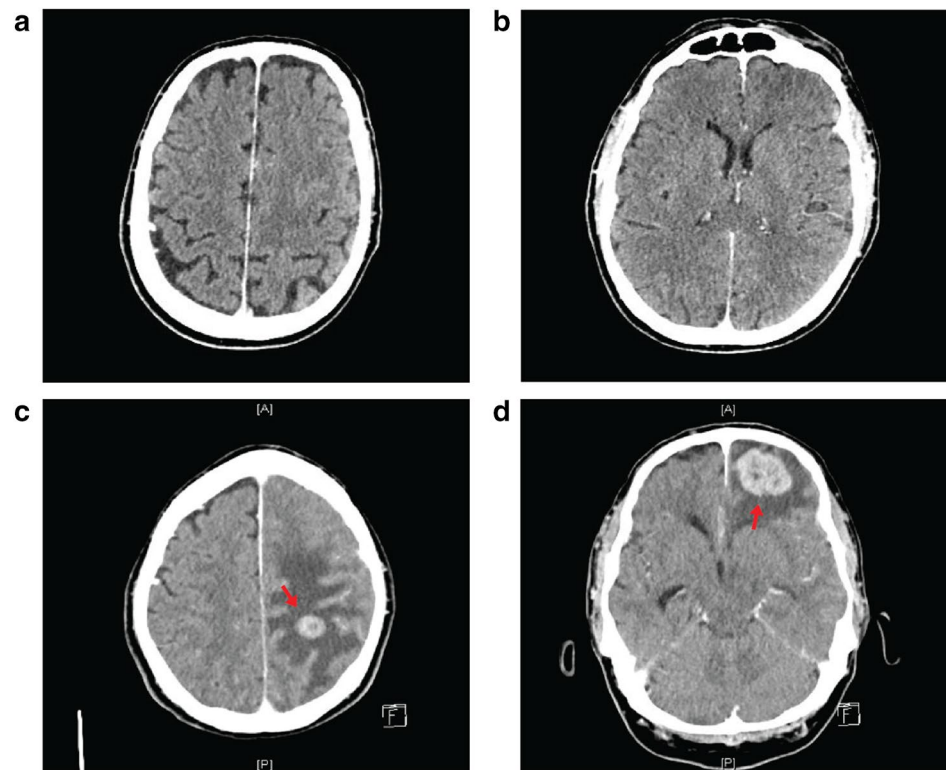
Lymphocyte, neutrophil and white blood cell (WBC) counts from the 1st of January to the 6th of September were collected via the electronic medical records at Liverpool Hospital. The neutrophil-to-lymphocyte ratio (NLR) was calculated by dividing the absolute neutrophil count by the absolute lymphocyte count.

Immunohistochemistry

One formalin-fixed, paraffin-embedded tissue test section was stained for PD-L1 (clone 22C3), using the PD-L1 IHC 22C3 PhamDx kit (supplied by SK006 DAKO North America, Inc.) with routine positive and negative control sections. The *BRAF V600E* immunostaining was performed on formalin-fixed, paraffin-embedded tissue sections against positive controls, loaded onto a Leica Bond III Immuno-autostainer at 1:250 (clone VE1, Spring Bioscience).

Mass cytometry immunophenotyping

PBMCs were processed using previously published methods [23].

Bacterial composition assessment by high-throughput sequencing

Faecal samples were collected at baseline and 4 weeks following treatment initiation. DNA extraction from 100 mg

of faeces was performed using the commercially available Power Fecal DNA isolation Kit (MO BIO, #12830-50) according to the manufacturer's protocol. DNA integrity was assessed by 1% agarose gel electrophoresis. Primers 0008F (5′-AGAGTTTGATCCTGGCTCAG-3′) and 0532R (5′-TAC CGCGGCTGCTGGCAC-3′) were used to amplify the first 500 bp of the 16S rRNA gene [24]. DNA was submitted to the Western Sydney University Next Generation Sequencing Facility for analysis. All DNA samples were initially purified using the Agencourt AMPure XP Beads (Beckman Coulter) followed by the quality and quantity assessment using the Lab Chip DS (Perkin Elmer) and the Quant-iT™ Pico-Green (Thermo Fisher Scientific), respectively. The primer set 27F/519R targeting the V1–V3 region of 16S gene was used for metagenomic sequencing [25]. The final libraries were run on Illumina MiSeq platform using a paired-end 2×300 bp sequencing.

Microbiome analysis

16S rDNA amplicons were processed using the QIIME2 pipeline (qiime2.org [26]) as follows: individual sequence variants (sOTUs) were identified using the DADA2 denoising package [27] which also merged paired sequences, removed chimeric sequences and reads with ambiguous bases. Taxonomy was assigned to sOTUs using the Q2 implementation [28] of a scikit-learn naive Bayes machine learning classifier [29] trained using the Greengenes

database V13_8 [30] and exported as relative abundance data. To ensure even sampling depth, samples were rarefied to 21186 reads. Alpha diversity metrics (sOTU richness and the Simpsons Index) were calculated using the 'diversity' package of QIIME2.

Results

Neutrophil-to-lymphocyte ratio

Neutrophil-to-lymphocyte ratio (NLR), a marker of systemic inflammation, is a strong prognostic marker in several cancer types [31–34]. Recently, two meta-analyses confirmed that an elevated pre-treatment NLR is associated with poorer outcomes in cancer patients receiving immunotherapy [35, 36]. Levels of circulating WBCs, lymphocytes and neutrophils during and following treatment cessation are illustrated in Fig. 4. After an initial drop to below 1×10^9 cells/L (NLR = 26.2), levels of circulating lymphocytes increased and remained within normal levels both during and 3 months following pembrolizumab treatment (Fig. 4b). Throughout this period, the patient had no evidence of disease progression. In contrast, pre-therapy levels of neutrophils were nearly twice the upper limit of normal (Fig. 4c). During treatment, neutrophil counts declined and remained within the normal range (NLR = 2.11). Interestingly, 1 month following the final dose of pembrolizumab, the patient's neutrophil count rebounded from 3.8×10^9ng/L to 7.4×10^9ng/L, and remained above the normal range preceding the detection of cerebral metastases by CT. Lymphocyte levels also reduced significantly at the time of cerebral metastases. The patient's levels of WBCs, lymphocytes and neutrophils fluctuated following his bowel perforation, and for the remainder of the follow-up period.

Blood lymphocyte studies

Immunophenotyping of PBMCs was performed using cryopreserved samples collected prior to commencing pembrolizumab, and at four time points during treatment. Compared to nine age- and sex-matched control subjects, the patient demonstrated a baseline elevation in CD45RO⁻ CCR7⁻ effector CD8⁺ T cells, consistent with the development of a T-cell-mediated immune response (Fig. 5a). Regulatory T cells (Tregs) expressing the transcription factor Foxp3 and low levels of CD127 were also prevalent both prior to and following immunotherapy (Fig. 5a).

The patient's pre-treatment CD20⁺ B cells were reduced more than threefold compared to controls. However, during treatment, a dramatic rise in B lymphocytes was observed, expanding more than fivefold (Fig. 5b, c). A marked

elevation in circulating CD16⁺ Cd56ˡᵒ NK cells was also detected. Whilst patient pre-treatment proportions of CD16⁺ NK cells were reduced threefold, by the final sample, they reached levels similar to healthy controls (Fig. 5b, c).

An increase in CD45RO⁺ CCR7⁺ central memory CD4⁺ T cells, PD-L1⁺ plasmacytoid dendritic cells (pDCs), CD4⁺ CD8⁺ double-positive T cells and HLA-DR +/CD14/ CD11c myeloid dendritic cells (mDCs) was also observed (Fig. 5b, c). Proportions of cells expressing TIGIT, a coinhibitory receptor, and OX40, a co-stimulatory receptor, also increased within CD8⁺, CD4⁺, Tregs and NK cells throughout the follow-up period. Moreover, mDCs, pDCs and monocytes all displayed increased expression of the co-stimulatory receptor CD86 during treatment (Fig. 5b).

Microbiome analysis

Faecal samples were collected prior to and at 1-month post-treatment. Taxonomic profiling using 16S ribosomal RNA (rRNA) gene sequencing was performed. The main bacterial phyla *Firmicutes* and *Bacteroidetes* remained relatively stable across the two time points (Fig. 6c). A high abundance of bacteria of the order *Bacteroidales*, specifically from the *Bacteroidaceae* and *Rikenellaceae* families, was identified in the faecal microbiota (Fig. 6b). Moreover, the patient's microbiome was enriched in *Clostridiales* order members *Ruminococcaceae*, *Veillonellaceae* and *Lachnospiraceae* (Fig. 6b). Alpha diversity (within-sample diversity) of the gut microbiome was significantly higher following initiation of checkpoint therapy as assessed by the Shannon and Simpson index (Fig. 6d). Whilst bacterial genera proportions differed between time points, they were not significantly altered by pembrolizumab treatment (Fig. 6a).

Discussion

We describe a patient with stage IVC ATC who experienced a radiographic response following four doses of pembrolizumab. The patient demonstrated a 53% reduction in total tumour burden, and during the follow-up period, his liver metastases continued to reduce in size. However, cerebral metastases were identified in a brain CT 8 months after the initiation of therapy.

Brain metastases are a significant predictor of death and disease progression following treatment with immune checkpoint blockade [37]. The inferior central nervous system (CNS) control exhibited by checkpoint inhibitors may result from their limited ability to penetrate the blood brain barrier (BBB) [38, 39]. However, inflammation and tumourigenesis may compromise the integrity of the BBB, allowing therapeutic agents and peripherally activated T cells into the tumour microenvironment [40]. Whilst immunotherapy as
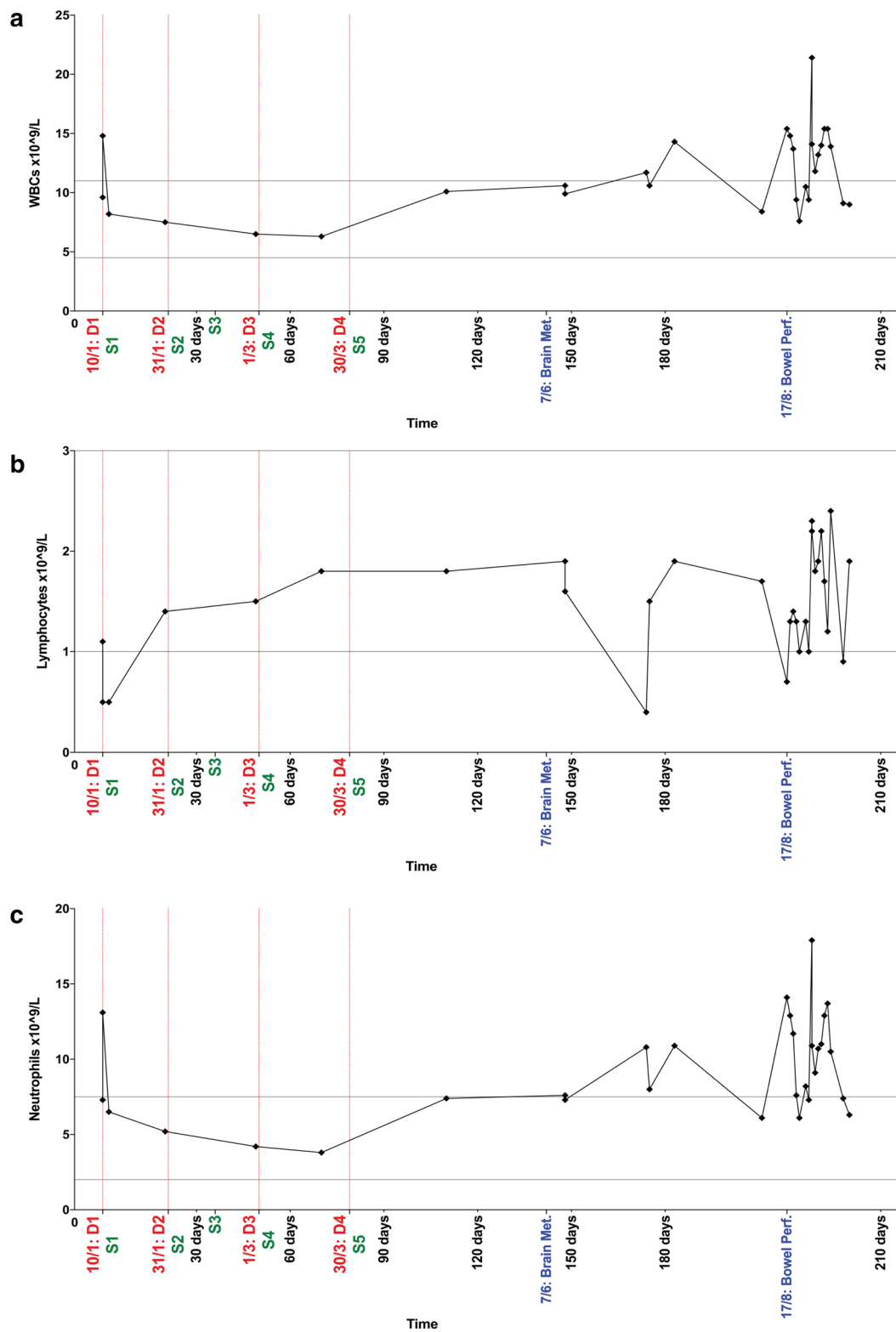
Fig. 4 Longitudinal levels ($\times 10^9$/L blood) of white blood cells (WBCs) (**a**) lymphocytes (**b**) and neutrophils (**c**) in ATC patient treated with pembrolizumab. Date of dose administration is indicated by the vertical red dotted lines. Normal value ranges are indicated by the horizontal grey lines (WBCs: 4.5–11 $\times 10^9$/L (**a**), lymphocytes: 1–3 $\times 10^9$/L (**b**), neutrophils: 2–7 $\times 10^9$/L (**c**)). Clinically significant events have been included on the x-axis. D dose. S sample collection
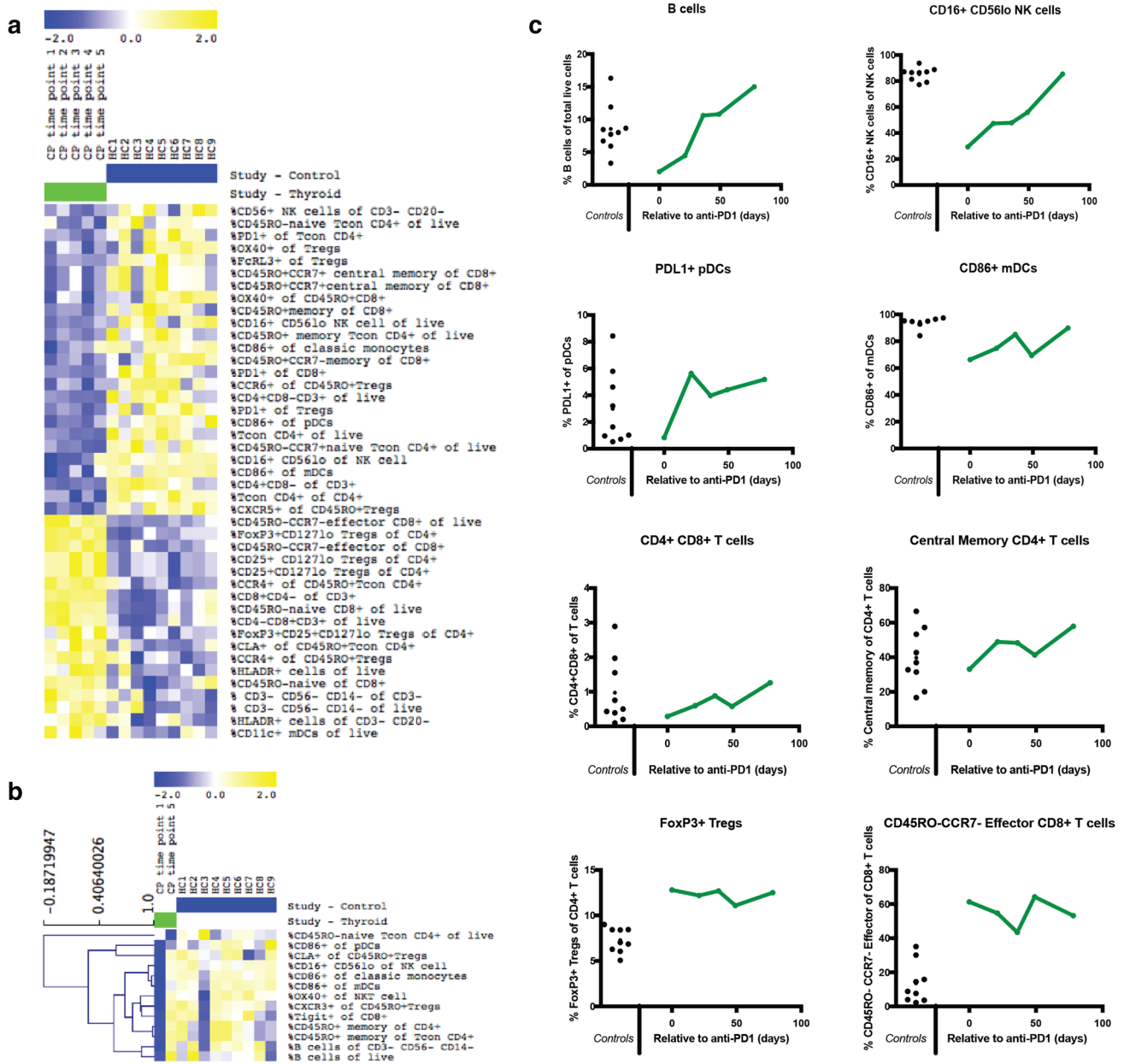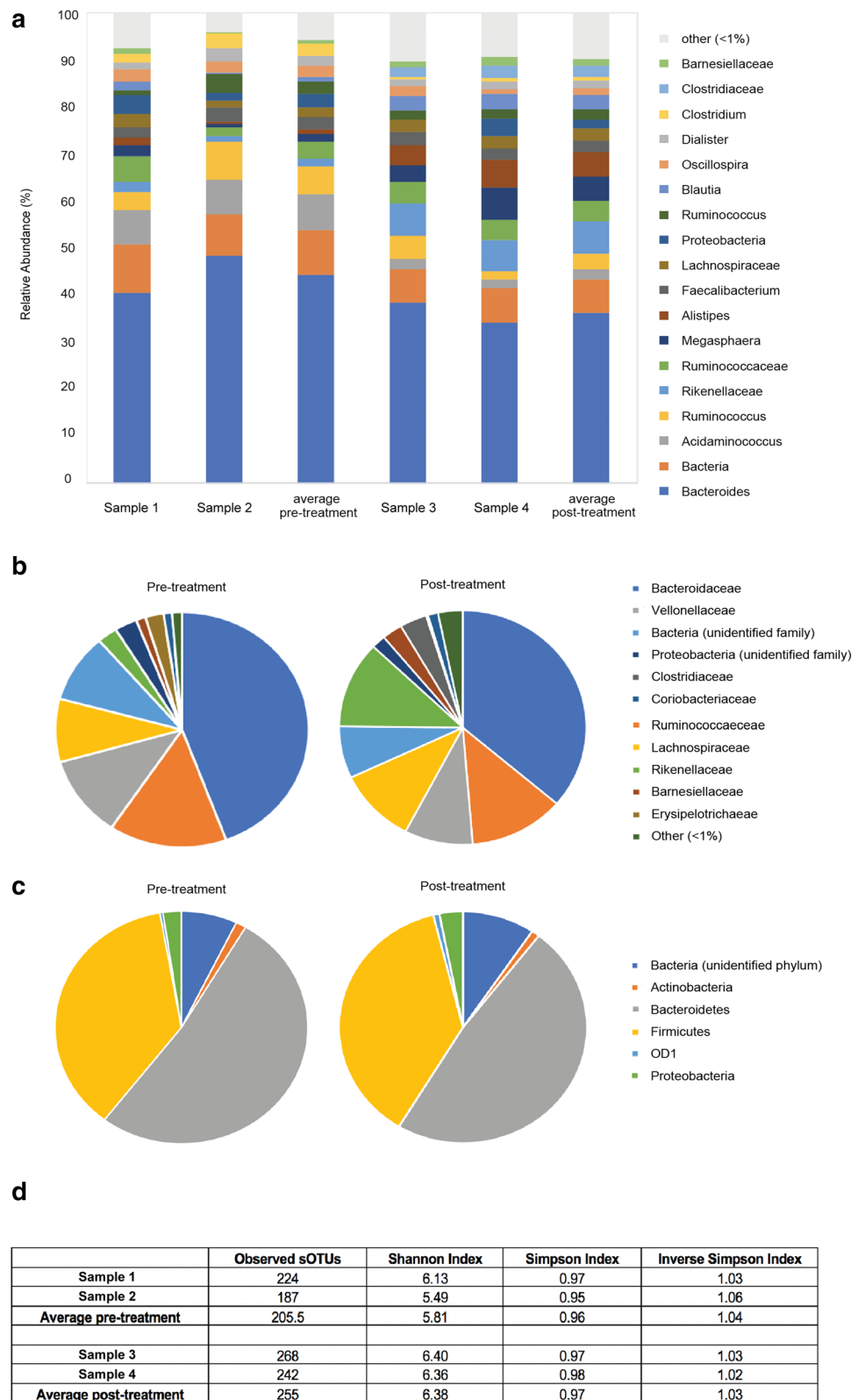
Fig. 5 Longitudinal monitoring of peripheral blood subsets in the ATC patient (**a**, **b**) Heat map of immunophenotyping results from patient time points (green) versus healthy controls (blue). Yellow indicates relative marker overexpression, blue indicates relative underexpression. **c** Longitudinal monitoring of peripheral blood subsets in the ATC patient. B cell, NK cell, pDC cell, mDC cell and T-cell subsets expressed as percentage of lymphocytes, calculated from mass cytometic analysis of longitudinal samples from the patient

monotherapy appears to have limited efficacy in cerebral metastases, the combination of immune modulators with additional therapies has yielded promising results [41]. In a recent trial, an intracranial response was observed in 16 (46%) of 35 melanoma patients with asymptomatic untreated brain metastases receiving nivolumab and ipilimumab, compared with only 5 (20%) of 25 patients treated with nivolumab monotherapy [42]. All patients on nivolumab monotherapy experienced intracranial progression whether alone or concurrently with extracranial progression. However, these results may not be generalisable to patients with symptomatic brain metastases, or those requiring corticosteroids for symptomatic control, as for our patient. The use of corticosteroids prior to and during treatment with immune checkpoint blockade has been associated with poorer outcomes, and may limit the efficacy of these immunotherapies in patients with brain metastases [43]. Additional studies are required to validate the use of immunotherapy as

Fig. 6 Differences in the gut microbiome prior to and during treatment with immunotherapy. **a** Main bacterial genera proportions prior to (Sample 1 and Sample 2) and 1 month into (Sample 3 and Sample 4) the commencement of pembrolizumab treatment. Only bacterial genera representing more than 1% of total reads on average are represented. **b** Bacterial family proportions pre- and post-treatment. **c** Bacterial phyla proportions pre- and post-treatment. **d** Observed sub-operational taxonomic units (sOTUs), Shannon Index, Simpson Index and Inverse Simpson Index prior to (Sample 1 and Sample 2) and 1 month into (Sample 1 and Sample 2) the commencement of pembrolizumab treatment

	Observed sOTUs	Shannon Index	Simpson Index	Inverse Simpson Index
Sample 1	224	6.13	0.97	1.03
Sample 2	187	5.49	0.95	1.06
Average pre-treatment	205.5	5.81	0.96	1.04
Sample 3	268	6.40	0.97	1.03
Sample 4	242	6.36	0.98	1.02
Average post-treatment	255	6.38	0.97	1.03

a monotherapy and in combination with other treatment modalities for improving outcomes amongst patients with brain metastases.

Immune cell subsets in pre- and post-therapy blood samples have been correlated with certain outcomes to checkpoint inhibition [23, 44–46]. We analysed peripheral blood

immune cells via mass cytometry to identify biomarker(s) predictive of clinical response to PD-1 blockade in ATC. During treatment, B cells, NK cells, pDCs, and central memory CD4^{+} T cells all increased in frequency. An increase in circulating classical monocytes expressing CD86 was also observed.

B cells are required for optimal T-cell activation and subsequent tumour regression [47, 48]. Chen et al. identified a B cell-derived expression signature predictive of response to immune checkpoint inhibitors in melanoma and urothelial carcinoma patients [49]. On multivariate analysis, this signature was the only independent predictor of patient response to treatment, whilst other biomarkers such as tumour mutation burden and PD-L1 expression remained non-significant. However, B cell populations with regulatory functions (Bregs) can either directly attenuate anti-tumour immunity via IL-10 secretion or indirectly compromise anti-tumour immunity through production of TGFβ and the conversion of resting CD4^{+} T cells into Tregs [50]. Many studies documenting Breg functions were performed using xenografts in mice where the immune system developed in the complete absence of B cells, potentially limiting their clinical relevance. Collectively, these findings suggest that the depletion and enhancement of particular B cell populations may be of therapeutic value in cancer patients. Additional research identifying phenotypic markers that can distinguish between pro- and anti-tumorigenic B cells, and the conditions that regulate these subsets are needed.

NK cells are key effectors of anticancer immunity, capable of eliminating malignantly transformed cells without prior immunisation [51]. Functional deficiency of NK cells has been associated with an increased risk of developing various types of cancer [52]. Moreover, NK cell effector functions are often impaired in cancer patients, with the extent of such dysfunction correlating with clinical prognosis [53]. In patients with relapsed or refractory Hodgkin's lymphoma (HL) treated with pembrolizumab, a significant treatment-induced expansion of T and NK cells was observed [54]. An increased frequency of CD56^{dim} NK cells (mature NK cells with a high cytotoxic activity) was associated with improved survival in 67 melanoma patients receiving anti-CTLA-4 treatment [55]. We similarly observed a threefold elevation in circulating CD16^{+} CD56^{lo} NK cells during the period of patient response. Thus, NK cells may provide a valuable biomarker indicative of ongoing antitumor activity and patient response to treatment.

In the absence of a specific stimulus, recruitment of pDCs to tumours has been associated with an immunosuppressive microenvironment and poor patient prognosis [56–58]. However, in mice, pDCs could effectively induce anti-tumour CD8^{+} T-cell responses when appropriately stimulated [59]. Type I IFN derived from pDCs regulates long-term T-cell survival and memory Th1 polarisation, CD8^{+} T-cell

cytotoxicity, and IFNγ production [59]. pDCs also increase NK cell-mediated cytotoxicity, induce differentiation and maturation of mDCs, and together with IL-6, prompt the differentiation of B lymphocytes into immunoglobulin-secreting plasma cells [59]. In our patient, increasing levels of circulating pDCs may indicate that more are available in the lymph node to enhance the induction of tumour-specific T cells.

CD4^{+} T cells promote tumour regression through multiple mechanisms, including IL-2 secretion, augmentation of tumour-specific CD8^{+} T-cell function, or direct elimination of cancer cells [60]. An increase in the proportion of CD27^{+}Fas^{−} central memory CD4^{+} T cells was detected by both mass cytometry and flow cytometry in the peripheral blood of malignant melanoma patients who responded clinically to PD-1 blockade therapy [61]. The expansion of central memory CD4^{+} T cells observed in our patient was associated with a clear anti-tumour response, and may be predictive of better survival outcomes in patients with ATC and potentially other tumours.

Interestingly, an increased frequency of circulating FoxP3^{+} regulatory T cells was associated with improved progression-free survival (PFS) in patients receiving neo-adjuvant ipilimumab for melanoma [62]. Moreover, Spitzer et al. reported that a subset of Tregs was elevated in responders 6 weeks following therapy commencement [63]. These expanded Tregs expressed lower levels of CD127 compared to the remaining CD4^{+} T cells, indicative of activation, and lower levels of PD-1, suggesting that they were not exhausted. Our patient demonstrated elevated levels of CD127^{lo} CD25^{+} FoxP3^{+} regulatory T cells both prior to and throughout pembrolizumab treatment. Similarly, no change in Tregs was observed in melanoma and breast cancer patients treated with pembrolizumab, whilst intratumoral CD8^{+} T memory cells expanded significantly [64, 65]. These results provide evidence of a critical role for CD4^{+} T cells in coordinating effective anti-tumour immunity; however, additional research is necessary to further delineate the role of Tregs following pembrolizumab treatment. Overall indicators of a 'normal' healthy immune system either prior to or in response to treatment may be more important than individual subset changes in predicting patient outcomes.

Whilst single-agent anti-PD-1/PD-L1 therapies have demonstrated promising clinical activity, response rates of 20% or less have been reported in several cancer types, including breast, RCC, and prostate cancer [66]. Our findings suggest that single-agent immunotherapy may be insufficient in the treatment of *BRAF*-negative stage IVC ATC. The efficacy of anti-PD1/PD-L1 treatment may be improved by simultaneously modulating other co-stimulatory and co-inhibitory receptors [67] or combined activation of the innate immune system [68]. In our patient, TIGIT increased in expression throughout the follow-up period. TIGIT is an important

coinhibitory receptor expressed on activated T cells, NK cells, memory T cells, Tregs and follicular T-helper (Tfh) cells [69]. Dual blockade of TIGIT and PD-1 synergistically stimulates immune cell proliferation, cytokine production, degranulation, and reversal of CD8$^+$ T-cell exhaustion with subsequent tumour rejection and induction of protective memory responses [70].

The co-stimulatory receptor OX40 also increased in expression in our patient, specifically on CD8$^+$, CD4$^+$, Tregs and NK cells. Agonists of activating immune checkpoints such as OX40 enhance T-cell proliferation, cytokine production, survival, and memory development. In a phase I study, increased proliferation of both CD4$^+$ and CD8$^+$ T cells was observed following treatment with anti-OX40 antibody, with 40% of cases experiencing tumour shrinkage of at least one metastatic lesion [71]. MOXR 0916, a humanised IgG agonistic monoclonal OX40-specific antibody, demonstrated no dose-limiting toxicities in combination with atezolizumab in patients with advanced solid malignancies (NCT02410512) [72]. By targeting these co-stimulatory and inhibitory pathways as they are detected in real-time during anti-PD1/PD-L1 treatment, clinicians may be able to overcome instances of innate or acquired resistance and improve patient outcomes. Multiple other combination therapies, including chemotherapy, radiotherapy and targeted therapies, also hold great promise in improving outcomes in patients unresponsive to single-agent treatment [73]. Whilst combination therapy has the potential to enhance therapeutic responses, it may also increase the likelihood for immune-related adverse events (irAEs) [74]. Future clinical trials will be necessary to determine whether combination therapies targeting other inhibitory pathways can successfully overcome resistance in ATC patients and provide additional clinical benefit.

Numerous studies have demonstrated the role of the gut microbiome in modulating patient responses to immune checkpoint blockade [75–77]; however, contradictory findings have been reported (Supplementary Table 1). Our patient demonstrated a significant increase in alpha microbial diversity following treatment with pembrolizumab. Improved PFS rates and enhanced immune checkpoint blockade efficacy were observed in melanoma, lung, renal, and bladder cancer patients with increased microbial diversity at baseline [75, 78]. Loss of microbial diversity (dysbiosis) has been associated with poorer outcomes following treatment with certain forms of cancer therapy. Antibiotic usage prior, during or shortly following the initiation of treatment with immune checkpoint blockade, significantly reduced PFS and overall survival (OS) in NSCLC and RCC patients [75]. Taxonomic profiling revealed that our patient's microbiome was enriched in *Clostridiales* order members *Ruminococcaceae*, *Veillonellaceae* and *Lachnospiraceae*. Potentially, an unleashed

T-cell response following immune checkpoint blockade could reshape gut microbial communities, change the number and proportion of some specific bacteria, and alter the function of bacterial species. Research aimed at understanding the function of different gut microbiome species, specific metabolic pathways activated by each species and the underlying mechanisms by which certain commensals interact with the immune system will allow us to potentially manipulate the human gut microbiome to improve patient response to checkpoint inhibitors.

In summary, we have described a patient with *BRAF*-negative stage IVC ATC who experienced a partial response following four doses of the PD-1 inhibitor pembrolizumab. Given the primary treatment resistance displayed by the tumour to chemoradiation in this patient, we speculate that PD-1 inhibition may have prolonged survival (16 months vs. a median of 5 months from the literature [79, 80]). Consistent with the findings of earlier studies, treatment promoted the expansion of T, B and NK cell populations in the peripheral blood at the time of tumour regression. Such expansions have the potential to be used as predictive biomarkers during checkpoint blockade therapy. We demonstrate how serial biopsies can provide an ongoing picture of an individual patient's molecular and microbiome profile prior to and throughout the course of treatment. Ultimately, this profile could be used by clinicians to make appropriate initial treatment decisions, devise rational combination strategies and overcome acquired resistance. Future studies using larger cohorts should prospectively evaluate the use of candidate biomarkers to predict patient response to treatment.

Compliance with ethical standards

Oncology Education and Research Translation (CONCERT) Biobank, in accordance with relevant legislation [81].

Informed consent Written informed consent was obtained from the patient who is the subject of the case study on January 10th, 2018. The patient agreed to the publication of this case study and the use of their specimens (provided that the participant could not be identified). Written informed consent was obtained from all controls prior to the study.

References

1. Taccaliti A, Silvetti F, Palmonella G, Boscaro M (2012) Anaplastic thyroid carcinoma. Front Endocrinol 3:84

2. Cornett WR, Sharma AK, Day TA, Richardson MS, Hoda RS, van Heerden JA et al (2007) Anaplastic thyroid carcinoma: an overview. Curr Oncol Rep 9(2):152–158

3. Nagaiah G, Hossain A, Mooney CJ, Parmentier J, Remick SC (2011) Anaplastic thyroid cancer: a review of epidemiology, pathogenesis, and treatment. J Oncol 2011:542358

4. Denaro N, Nigro CL, Russi EG, Merlano MC (2013) The role of chemotherapy and latest emerging target therapies in anaplastic thyroid cancer. Oncol Targets Therp 9:1231–1241

5. Ayaz T, Sahin SB, Sahin OZ, Akdogan R, Gücer R (2015) Anaplastic thyroid carcinoma presenting with gastric metastasis: a case report. Hippokratia. 19(1):85–87

6. Besic N, Gazic B (2013) Sites of metastases of anaplastic thyroid carcinoma: autopsy findings in 45 cases from a single institution. Thyroid 23(6):709–713

7. Stavas MJ, Shinohara ET, Attia A, Ning MS, Friedman JM, Cmelak AJ (2014) Short course high dose radiotherapy in the treatment of anaplastic thyroid carcinoma. J Thyroid Res 2014:764281

8. Rao SN, Zafereo M, Dadu R, Busaidy NL, Hess K, Cote GJ et al (2017) Patterns of treatment failure in anaplastic thyroid carcinoma. Thyroid 27(5):672–681

9. Prasongsook N, Kumar A, Chintakuntlawar AV, Foote RL, Kasperbauer J, Molina J et al (2017) Survival in response to multimodal therapy in anaplastic thyroid cancer. J Clin Endocrinol Metab 102(12):4506–4514

10. Keir ME, Butte MJ, Freeman GJ, Sharpe AH (2008) PD-1 and its ligands in tolerance and immunity. Annu Rev Immunol 26:677–704

11. Bardhan K, Anagnostou T, Boussiotis VA (2016) The PD1:PD-L1/2 pathway from discovery to clinical implementation. Front Immunol 7:550

12. Topalian SL, Hodi FS, Brahmer JR, Gettinger SN, Smith DC, McDermott DF et al (2012) Safety, activity, and immune correlates of anti–PD-1 antibody in cancer. N Engl J Med 366(26):2443–2454

13. Borcherding N, Kolb R, Gullicksrud J, Vikas P, Zhu Y, Zhang W (2018) Keeping tumors in check: a mechanistic review of clinical response and resistance to immune checkpoint blockade in cancer. J Mol Biol 430(14):2014–2029

14. Iyer PC, Dadu R, Gule-Monroe M, Busaidy NL, Ferrarotto R, Habra MA et al (2018) Salvage pembrolizumab added to kinase inhibitor therapy for the treatment of anaplastic thyroid carcinoma. J Immunotherap Cancer 6(1):68

15. Kollipara R, Schneider B, Radovich M, Babu S, Kiel PJ (2017) Exceptional response with immunotherapy in a patient with Anaplastic Thyroid Cancer. Oncologist 22(10):1149–1151. https://doi.org/10.1634/theoncologist.2017-0096

16. Wirth LJ, Eigendorff E, Capdevila J, Paz-Ares LG, Lin C-C, Taylor MH et al (2018) Phase I/II study of spartalizumab (PDR001), an anti-PD1 mAb, in patients with anaplastic thyroid cancer. J Clin Oncol 36(15_suppl):6024

17. Chintakuntlawar A, Yin J, Foote RL, Kasperbauer JL, Rivera M, Asmus E, Garces N, Janus J, Ma DJ, Moore EJ, Morris J, Neben-Wittich M, Price D, Ryder M, Van Abel K, Hilger CR, Samb E, Bible K (2018) A phase 2 study of pembrolizumab combined with chemoradiotherapy as initial treatment for anaplastic thyroid cancer. In: 88th Annual Meeting of the American Thyroid Association Washington, DC

18. Horn L, Spigel DR, Vokes EE, Holgado E, Ready N, Steins M et al (2017) Nivolumab versus docetaxel in previously treated patients with advanced non-small-cell lung cancer: 2-year outcomes from two randomized, open-label, phase III trials (CheckMate 017 and CheckMate 057). J Clin Oncol 35(35):3924–3933

19. Motzer RJ, Escudier B, McDermott DF, George S, Hammers HJ, Srinivas S et al (2015) Nivolumab versus everolimus in advanced renal-cell carcinoma. N Engl J Med 373(19):1803–1813

20. Robert C, Long GV, Brady B, Dutriaux C, Maio M, Mortier L et al (2015) Nivolumab in previously untreated melanoma without BRAF mutation. N Engl J Med 372(4):320–330

21. Borghaei H, Paz-Ares L, Horn L, Spigel DR, Steins M, Ready NE et al (2015) Nivolumab versus docetaxel in advanced nonsquamous non-small-cell lung cancer. N Engl J Med 373(17):1627–1639

22. Maleki Vareki S, Garrigos C, Duran I (2017) Biomarkers of response to PD-1/PD-L1 inhibition. Crit Rev Oncol Hematol 116:116–124

23. McGuire HM, Shklovskaya E, Edwards J, Trevillian PR, McCaughan GW, Bertolino P et al (2018) Anti-PD-1-induced high-grade hepatitis associated with corticosteroid-resistant T cells: a case report. Cancer Immunol Immunotherap CII 67(4):563–573

24. Imrit K, Goldfischer M, Wang J, Green J, Levine J, Lombardo J et al (2006) Identification of bacteria in formalin-fixed, paraffin-embedded heart valve tissue via 16S rRNA gene nucleotide sequencing. J Clin Microbiol 44(7):2609–2611

25. Handl S, Dowd SE, Garcia-Mazcorro JF, Steiner JM, Suchodolski JS (2011) Massive parallel 16S rRNA gene pyrosequencing reveals highly diverse fecal bacterial and fungal communities in healthy dogs and cats. FEMS Microbiol Ecol 76(2):301–310

26. Caporaso JG, Kuczynski J, Stombaugh J, Bittinger K, Bushman FD, Costello EK et al (2010) QIIME allows analysis of high-throughput community sequencing data. Nat Methods 7(5):335–336

27. Callahan BJ, McMurdie PJ, Rosen MJ, Han AW, Johnson AJ, Holmes SP (2016) DADA2: high-resolution sample inference from Illumina amplicon data. Nat Methods 13(7):581–583

28. Bokulich NA, Kaehler BD, Rideout JR, Dillon M, Bolyen E, Knight R et al (2018) Optimizing taxonomic classification of marker-gene amplicon sequences with QIIME 2′s q2-feature-classifier plugin. Microbiome 6(1):90

29. Pedregosa F, Varoquaux G, Gramfort A, Michel V, Thirion B, Grisel O, Vanderplas J (2011) Scikit-learn: machine learning in Python. J Mach Learn Res 12:2825–2830

30. McDonald D, Price MN, Goodrich J, Nawrocki EP, DeSantis TZ, Probst A et al (2012) An improved Greengenes taxonomy with explicit ranks for ecological and evolutionary analyses of bacteria and archaea. ISME J 6(3):610–618

31. Li MX, Liu XM, Zhang XF, Zhang JF, Wang WL, Zhu Y et al (2014) Prognostic role of neutrophil-to-lymphocyte ratio in colorectal cancer: a systematic review and meta-analysis. Int J Cancer 134(10):2403–2413

32. Paramanathan A, Saxena A, Morris DL (2014) A systematic review and meta-analysis on the impact of pre-operative neutrophil lymphocyte ratio on long term outcomes after curative intent resection of solid tumours. Surg Oncol 23(1):31–39

33. Templeton AJ, McNamara MG, Seruga B, Vera-Badillo FE, Aneja P, Ocana A et al (2014) Prognostic role of neutrophil-to-lymphocyte ratio in solid tumors: a systematic review and meta-analysis. J Natl Cancer Inst 106(6):dju124

34. Ding PN, Roberts TL, Chua W, Becker TM, Descallar J, Yip PY et al (2017) Clinical outcomes in patients with advanced epidermal growth factor receptor-mutated non-small-cell lung cancer in South Western Sydney Local Health District. Int Med J 47(12):1405–1411

35. Sacdalan DB, Lucero JA, Sacdalan DL (2018) Prognostic utility of baseline neutrophil-to-lymphocyte ratio in patients receiving immune checkpoint inhibitors: a review and meta-analysis. OncoTargets Therap 11:955–965

36. Tan Q, Liu S, Liang C, Han X, Shi Y (2018) Pretreatment hematological markers predict clinical outcome in cancer patients receiving immune checkpoint inhibitors: a meta-analysis. Thoracic Cancer. 9(10):1220–1230

37. Cowey CL, Liu FX, Black-Shinn J, Stevinson K, Boyd M, Frytak JR et al (2018) Pembrolizumab utilization and outcomes for advanced melanoma in US community oncology practices. J Immunotherap (Hagerstown MD 1997) 41(2):86–95

38. Dang TO, Ogunniyi A, Barbee MS, Drilon A (2016) Pembrolizumab for the treatment of PD-L1 positive advanced or metastatic non-small cell lung cancer. Expert Rev Anticancer Ther 16(1):13–20

39. Fonkem E, Uhlmann EJ, Floyd SR, Mahadevan A, Kasper E, Eton O et al (2012) Melanoma brain metastasis: overview of current management and emerging targeted therapies. Expert Rev Neurother 12(10):1207–1215

40. Silk AW, Bassetti MF, West BT, Tsien CI, Lao CD (2013) Ipilimumab and radiation therapy for melanoma brain metastases. Cancer Med 2(6):899–906

41. Tallet AV, Dhermain F, Le Rhun E, Noël G, Kirova YM (2017) Combined irradiation and targeted therapy or immune checkpoint blockade in brain metastases: toxicities and efficacy. Ann Oncol 28(12):2962–2976

42. Long GV, Atkinson V, Lo S, Sandhu S, Guminski AD, Brown MP et al (2018) Combination nivolumab and ipilimumab or nivolumab alone in melanoma brain metastases: a multicentre randomised phase 2 study. Lancet Oncol 19(5):672–681

43. Arbour KC, Mezquita L, Long N, Rizvi H, Auclin E, Ni A et al (2018) Impact of baseline steroids on efficacy of programmed cell death-1 and programmed death-ligand 1 blockade in patients with non-small-cell lung cancer. J Clin Oncol 36(28):2872–2878

44. Krieg C, Nowicka M, Guglietta S, Schindler S, Hartmann FJ, Weber LM et al (2018) High-dimensional single-cell analysis predicts response to anti-PD-1 immunotherapy. Nat Med 24:144

45. Lomax AJ, McGuire HM, McNeil C, Choi CJ, Hersey P, Karikios D et al (2017) Immunotherapy-induced sarcoidosis in patients with melanoma treated with PD-1 checkpoint inhibitors: case series and immunophenotypic analysis. Int J Rheumatic Dis 20(9):1277–1285

46. Kamphorst AO, Pillai RN, Yang S, Nasti TH, Akondy RS, Wieland A et al (2017) Proliferation of PD-1 + CD8 T cells in peripheral blood after PD-1–targeted therapy in lung cancer patients. Proc Natl Acad Sci 114(19):4993–4998

47. Yuseff MI, Pierobon P, Reversat A, Lennon-Dumenil AM (2013) How B cells capture, process and present antigens: a crucial role for cell polarity. Nat Rev Immunol 13(7):475–486

48. Guy TV, Terry AM, Bolton HA, Hancock DG, Shklovskaya E, de Fazekas SGB (2016) Pro- and anti-tumour effects of B cells and antibodies in cancer: a comparison of clinical studies and preclinical models. Cancer Immunol Immunother 65(8):885–896

49. Varn FS, Wang Y, Cheng C (2019) A B cell-derived gene expression signature associates with an immunologically active tumor microenvironment and response to immune checkpoint blockade therapy. Oncoimmunology 8(1):e1513440

50. Sarvaria A, Madrigal JA, Saudemont A (2017) B cell regulation in cancer and anti-tumor immunity. Cell Mol Immunol 14(8):662–674

51. Grossenbacher SK, Aguilar EG, Murphy WJ (2017) Leveraging natural killer cells for cancer immunotherapy. Immunotherapy 9(6):487–497

52. Imai K, Matsuyama S, Miyake S, Suga K, Nakachi K (2000) Natural cytotoxic activity of peripheral-blood lymphocytes and cancer incidence: an 11-year follow-up study of a general population. Lancet (Lond Engl) 356(9244):1795–1799

53. Kim HS (2015) A multifaceted approach targeting NK cells for better treatment of cancer: focus on hematological malignancies. Blood Res 50(4):189–191

54. Armand P, Shipp MA, Ribrag V, Michot JM, Zinzani PL, Kuruvilla J et al (2016) Programmed death-1 blockade with pembrolizumab in patients with classical hodgkin lymphoma after brentuximab vedotin failure. J Clin Oncol 34(31):3733–3739

55. Tallerico R, Cristiani CM, Staaf E, Garofalo C, Sottile R, Capone M et al (2017) IL-15, TIM-3 and NK cells subsets predict responsiveness to anti-CTLA-4 treatment in melanoma patients. Oncoimmunology 6(2):e1261242

56. Labidi-Galy SI, Treilleux I, Goddard-Leon S, Combes JD, Blay JY, Ray-Coquard I et al (2012) Plasmacytoid dendritic cells infiltrating ovarian cancer are associated with poor prognosis. Oncoimmunology 1(3):380–382

57. Jensen TO, Schmidt H, Moller HJ, Donskov F, Hoyer M, Sjoegren P et al (2012) Intratumoral neutrophils and plasmacytoid dendritic cells indicate poor prognosis and are associated with pSTAT3 expression in AJCC stage I/II melanoma. Cancer 118(9):2476–2485

58. Treilleux I, Blay JY, Bendriss-Vermare N, Ray-Coquard I, Bachelot T, Guastalla JP et al (2004) Dendritic cell infiltration and prognosis of early stage breast cancer. Clin Cancer Res 10(22):7466–7474

59. Pinto A, Rega A, Crother TR, Sorrentino R (2012) Plasmacytoid dendritic cells and their therapeutic activity in cancer. Oncoimmunology. 1(5):726–734

60. Lai Y-P, Jeng C-J, Chen S-C (2011) The roles of CD4 + T cells in tumor immunity. ISRN Immunol 2011:6

61. Takeuchi Y, Tanemura A, Tada Y, Katayama I, Kumanogoh A, Nishikawa H (2018) Clinical response to PD-1 blockade correlates with a sub-fraction of peripheral central memory CD4 + T cells in patients with malignant melanoma. Int Immunol 30(1):13–22

62. Tarhini AA, Edington H, Butterfield LH, Lin Y, Shuai Y, Tawbi H et al (2014) Immune monitoring of the circulation and the tumor microenvironment in patients with regionally advanced melanoma receiving neoadjuvant ipilimumab. PLoS One 9(2):e87705

63. Spitzer MH, Carmi Y, Reticker-Flynn NE, Kwek SS, Madhireddy D, Martins MM et al (2017) Systemic immunity is required for effective cancer immunotherapy. Cell 168(3):487–502.e15

64. Ribas A, Shin DS, Zaretsky J, Frederiksen J, Cornish A, Avramis E et al (2016) PD-1 blockade expands intratumoral memory T cells. Cancer Immunol Res 4(3):194–203

65. Toor SM, Syed Khaja AS, Alkurd I, Elkord E (2018) In-vitro effect of pembrolizumab on different T regulatory cell subsets. Clin Exp Immunol 191(2):189–197

66. Lipson EJ, Forde PM, Hammers H-J, Emens LA, Taube JM, Topalian SL (2015) Antagonists of PD-1 and PD-L1 in cancer treatment. Semin Oncol 42(4):587–600

67. Ott PA, Hodi FS, Kaufman HL, Wigginton JM, Wolchok JD (2017) Combination immunotherapy: a road map. J Immunother Cancer. 5:16

68. Li K, Qu S, Chen X, Wu Q, Shi M (2017) Promising Targets for Cancer Immunotherapy: TLRS, RLRs, and STING-mediated innate immune pathways. Int J Mol Sci 18(2):404

69. Kurtulus S, Sakuishi K, Ngiow SF, Joller N, Tan DJ, Teng MW et al (2015) TIGIT predominantly regulates the immune response via regulatory T cells. J Clin Investig 125(11):4053–4062

70. Anderson AC, Joller N, Kuchroo VK (2016) Lag-3, Tim-3, and TIGIT: co-inhibitory receptors with specialized functions in immune regulation. Immunity 44(5):989–1004

71. Curti BD, Kovacsovics-Bankowski M, Morris N, Walker E, Chisholm L, Floyd K et al (2013) OX40 is a potent immune-stimulating target in late-stage cancer patients. Can Res 73(24):7189–7198

72. Infante JR, Hansen AR, Pishvaian MJ, Chow LQM, McArthur GA, Bauer TM et al (2016) A phase Ib dose escalation study of the OX40 agonist MOXR0916 and the PD-L1 inhibitor atezolizumab in patients with advanced solid tumors. J Clin Oncol 34(15_suppl):101

73. Harris SJ, Brown J, Lopez J, Yap TA (2016) Immuno-oncology combinations: raising the tail of the survival curve. Cancer Biol Med 13(2):171–193

74. Puzanov I, Diab A, Abdallah K, Bingham CO 3rd, Brogdon C, Dadu R et al (2017) Managing toxicities associated with immune checkpoint inhibitors: consensus recommendations from the Society for Immunotherapy of Cancer (SITC) Toxicity Management Working Group. J Immunother Cancer. 5(1):95

75. Routy B, Le Chatelier E, Derosa L, Duong CPM, Alou MT, Daillere R et al (2018) Gut microbiome influences efficacy of PD-1-based immunotherapy against epithelial tumors. Science (New York, NY). 359(6371):91–97

76. Frankel AE, Coughlin LA, Kim J, Froehlich TW, Xie Y, Frenkel EP et al (2017) Metagenomic shotgun sequencing and unbiased metabolomic profiling identify specific human gut microbiota and metabolites associated with immune checkpoint therapy efficacy in melanoma patients. Neoplasia (New York, NY). 19(10):848–855

77. Vétizou M, Pitt JM, Daillère R, Lepage P, Waldschmitt N, Flament C et al (2015) Anticancer immunotherapy by CTLA-4 blockade relies on the gut microbiota. Science (New York, NY). 350(6264):1079–1084

78. Gopalakrishnan V, Spencer CN, Nezi L, Reuben A, Andrews MC, Karpinets TV et al (2018) Gut microbiome modulates response to anti-PD-1 immunotherapy in melanoma patients. Science (New York, NY). 359(6371):97–103

79. Derbel O, Limem S, Segura-Ferlay C, Lifante JC, Carrie C, Peix JL et al (2011) Results of combined treatment of anaplastic thyroid carcinoma (ATC). BMC Cancer 11:469

80. Seto A, Sugitani I, Toda K, Kawabata K, Takahashi S, Saotome T (2015) Chemotherapy for anaplastic thyroid cancer using docetaxel and cisplatin: report of eight cases. Surg Today 45:221–226

81. Caixeiro NJ, Aghmesheh, M., de Souza P, Lee, CS (2015) The Centre for Oncology Education and Research Translation (CONCERT) Biobank. Open J Bioresour 2(1):Art. e3. doi: http://doi.org/10.5334/ojb.ai

Publisher's Note Springer Nature remains neutral with regard to jurisdictional claims in published maps and institutional affiliations.